PNAS
www.pnas.org

Supplementary Information for

Loss of function of a DMR6 ortholog in tomato confers broad-spectrum disease resistance

Daniela Paula de Toledo Thomazella, Kyungyong Seong, Rebecca Mackelprang, Douglas Dahlbeck, Yu Geng, Upinder S. Gill, Tiancong Qi, Julie Pham, Priscila Giuseppe, Clara Youngna Lee, Arturo Ortega[1,4], Myeong-Je Cho, Samuel F. Hutton and Brian Staskawicz*

* To whom correspondence should be addressed.
Email: stask@berkeley.edu

This PDF file includes:

- Supplementary text
- Figures S1 to S13
- Table S1 and S2
- Captions for databases S1 to S5
- References for SI reference citations

Other supplementary materials for this manuscript include the following:

- Datasets S1 to S5

Supplementary Information Text

Materials and Methods

Phylogenetic analysis and data mining

To reconstruct the phylogenetic tree for the 2-oxoglutarate Fe(II) dependent oxygenase superfamily, we collected the sequences of functionally characterized proteins, namely AtDMR6, AtDLO1, AtDLO2, AtFLS, AtFH3, AtANS, AtACC and PcFNS. We searched with BLASTP their homologous sequences from angiosperm species with well-annotated genomes. They included the monocots corn (*Zea mays*), rice (*Oryza sativa*) and sorghum (*Sorghum bicolor*) and the dicots *Arabidopsis thaliana*, cacao (*Theobroma cacao*), cassava (*Manihot esculenta*), bean (*Phaseolus vulgaris*), lettuce (*Lactuca sativa*), papaya (*Carica papaya*), and some species from the Solanaceae family, including eggplant (*Solanum melongena*), pepper (*Capsicum annuum*), potato (*Solanum tuberosum*) and tomato (*Solanum lycopersicum*) (1). The matches that showed e-value of 1E-4 and 70% bi-directional coverages with the queries were retained. All the remaining sequences, together with the outgroup S7S0B0, were aligned with MAFFT v7.313 (--maxiterate 1000 –globalpair) (2). Columns with 80% or more gaps were removed. The resulting multiple sequence alignment was used to infer a maximum-likelihood tree using RAxML v8.2.12 (-p 12345 -# 100 -m PROTGAMMAWAGF) with 500 rapid bootstrap replications (3). Homologs that clustered with AtDMR6 were defined as DMR6 clade. We selected two tomato homologs SlDMR6-1 and SlDMR6-2 in the DMR6 clade for the study. Publicly available transcriptome data (4–6) were inspected for *SlDMR6-1* and *SlDMR6-2* expression in response to different pathogens, such as *Pseudomonas syringae* (bacteria), *Phytophthora capsici* (oomycete) and *Moniliophthora perniciosa* (fungus). In addition, we selected the cacao and cassava (Thecc1EG015521t1 and Manes.01G043500.1) *DMR6* orthologs, which were named *TcDMR6* and *MeDMR6*, respectively, and analyzed their expression in public transcriptomic data (7–9).

Promoter analysis

We collected 1-kb promoter regions of *SlDMR6-1* and *SlDMR6-2* from *Solanum lycopersicum*, *Solanum pennellii*, *Capsicum annuum*, *Capsicum baccatum*, *Petunia axillaris* and *Petunia inflata* from Sol Genomics (https://solgenomics.net). For each orthologous group, we performed conserved motif search with Multiple Expression motifs for Motif Elicitation (MEME) v5.0.5 (10). The UTRs of *SlDMR6-1* and *SlDMR6-2* were obtained from their cDNAs. We selected motifs predicted outside the UTRs and conserved in all six species. We ran TOMTOM to compare the predicted motifs to transcription binding sites available in JASPAR (11).

Biological material and growth conditions

For all experiments, we used the wild type plant Fla. 8000, which is susceptible to *Xanthomonas* (12). Wild type and mutant (*Sldmr6-1* and *Sldmr6-2*) plants were grown on soil (Miracle-Gro Supersoil Potting Soil) in a growth chamber at 25°C under a 16-h light/8-h dark photoperiod and 50% relative humidity. Experiments were performed with six-week-old plants. Experiments in which the mutant allele was not specified were performed with the mutants *Sldmr6-1.2* and *Sldmr6-2.2* as representatives of the genotypes *Sldmr6-1* and *Sldmr6-2*, respectively.

Pseudomonas syringae pv. *tomato* DC3000 (*Pst* DC3000), *Xanthomonas gardneri* 153 (Xg153), *X. perforans* 4B (Xp4B) were used for plant inoculation. *Agrobacterium tumefaciens* strains C58C1 and GV3101 were used for transient expression and tomato transformation, respectively. For pathogen assays, bacterial cultures were grown in NYG (peptone 5 g/l, yeast extract 3 g/l, glycerol 20 ml/l) for 18 h at 28°C on a shaker at 150 rpm. *Phytophthora capsici* (LT1534 isolate) was maintained at 25°C on either Rye A Agar in the dark for mycelial growth or 10% Unclarified V8 Agar in the light for sporangium formation. Spores of *Pseudoidium neolycopersici* (MF-1 isolate) were maintained and propagated on tomato Moneymaker plants in an isolated growth room at 25°C with a 12-h photoperiod.

Cas9-mediated inactivation of *SlDMR6-1* and *SlDMR6-2* genes

Two guide RNAs (gRNAs) were used for each of the target genes: *SlDMR6-1* (Solyc03g080190) and *SlDMR6-2* (Solyc06g073080). Each guide was independently cloned into a pENTR/D-TOPO-based entry plasmid containing the *Arabidopsis* U6-26 promoter to drive gRNA expression and a double 35S promoter driving Cas9 expression (13, 14). A gateway LR reaction (Thermo Fisher Scientific) was used to move the gRNA and Cas9 cassette into a pPZP200-based binary vector (15). Before proceeding to tomato transformation, gRNA activity was evaluated by *Agrobacterium*-mediated transient expression of the binary plasmid into *N. benthamiana* leaves as described before (13). Using the *Agrobacterium tumefaciens* co-cultivation method, the binary construct was used for transformation into the Fla. 8000 variety at the University of Nebraska Plant Transformation Core Research Facility (https://biotech.unl.edu/plant-transformation). Kanamycin-resistant plants were genotyped, and the selected mutants were selfed for the use in subsequent experiments. All primers are listed in Table S1.

RNA extraction and qRT-PCR (Quantitative Real-Time Polymerase Chain Reaction)

Leaf samples were collected 6 hours after syringe infiltration with *X. gardneri*. Total RNA was extracted using the Spectrum Plant Total RNA kit (Sigma, STRN250). Reverse transcription was performed with 1 µg total RNA, using the SuperScript III First-Strand Synthesis SuperMix for qRT-PCR (Invitrogen, 11752-250). Gene expression was quantified with the IQ SYBR Green

Supermix (BIO-RAD Cat. 1708882) on a BioRad CFX96 qPCR System. *SlAct* (Solyc03g078400) gene was used as internal control. Three biological replicates were used for each experimental condition. Primer sequences are listed in Table S1.

Pathogen assays

Bacteria were grown in NYG (0.5% peptone, 0.3% yeast extract, 2% glycerol) with 100 µg/ml rifampicin on a shaker at 200 rpm, at 28°C overnight. After centrifugation at 4,000 ×g for 15 min, cells were washed once with 10 mM $MgCl_2$, and diluted to OD_{600nm}=0.1 for infection assays. Plants were infected by dip inoculating three leaflets into the bacterial suspension amended with 0.02% Silwet L-77. Infected plants were grown on a 12-h photoperiod at 25°C until symptoms develop. Leaf punches were collected, homogenized and then serially diluted. For quantification of bacterial populations, serial dilutions of leaf homogenates were plated onto NYGA (0.5% peptone, 0.3% yeast extract, 2% glycerol, 1.5% agar) with 100 µg/ml rifampicin and 50 µg/ml cycloheximide. After incubation at 28°C for 4 to 5 days, typical colonies of *Xanthomonas* spp./*P. syringae* were counted, and the bacterial population on each genotype was estimated.

For *P. capsici* pathogen assay, isolate LT1534 was grown on V8 agar 10% at 25°C for three days in the dark and for additional two days under fluorescent light. For inoculation, a plate covered with mycelium was flooded with cold water and the zoospore suspension was obtained after 30 minutes at room temperature. Leaves were spot inoculated by pipetting 10 µl droplets of the spore suspension (10^5 spores/ml) on the adaxial side of each tomato leaflet.

P. neolycopersici assay was performed by evenly spraying fungal spores from infected branches on the aerial parts of the plants. Fungal growth was evaluated at 5 and 7 days after inoculation (dai). The terminal leaflet of the fifth true leaf was sampled, and its fresh weight was determined. Leaflets were individually placed in 50 ml falcon tubes with 20 ml H_2O, vortexed for 60 sec and filtered with Miracloth. The liquid was centrifuged at 3100 xg for 30 mins and the pellet was resuspended in 500 µl 50% glycerol. An aliquot (50 µl) was then used for counting the spores on an epifluorescence microscope.

Measurement of tomato growth

To evaluate the effect of *SlDMR6-1* and *SlDMR6-2* mutations on plant growth, the height of *Sldmr6-1*, *Sldmr6-2* and wild type plants (18 individuals from each genotype) was recorded using a tape measure (Stanley FatMax 25'). For this, seeds were sowed in supersoil potting soil (Miracle-Gro) and maintained in a growth chamber at 25°C, 16-h light/8-h dark photoperiod and 50% relative humidity. Shoot length was determined 30 days after seedling emergence by measuring the distance between the base of the cotyledon leaves and the apical meristem. Statistical significance

was assessed using a one-way ANOVA and post hoc Tukey's honestly significant difference (HSD) test ($p \leq 0.05$).

Promoter GUS transgenic lines and histochemical GUS staining

A 2.5-kb fragment including the putative *SlDMR6-1* promoter was amplified with specific primers (Table S1) and cloned via LR reaction into the gateway binary vector pGWB3 (16) to generate the *proSlDMR6-1:GUS* binary vector. The histochemical GUS assay was performed using a previously described method (17). Leaves from wild type and *proSlDMR6-1:GUS* lines were syringe infiltrated with staining buffer (0.5 mg/ml 5-bromo-4-chloro-3-indolyl glucuronide in 0.1 M Na_2HPO_4, pH 7 and 10 mM Na_2EDTA) and maintained at 37°C, overnight. After the staining buffer was removed, samples were cleared with 70% ethanol. Leaves were imaged with a handheld digital camera.

Salicylic acid (SA) analysis using liquid chromatography (LC)-MS/MS

Leaf samples of plants growing under laboratory conditions were collected 6 hours after syringe infiltration with *X. gardneri* suspension (OD_{600}= 0.25). Total SA (the sum of free SA and SA glucosides) was extracted from 100 mg of frozen leaf tissues, after the addition of appropriate internal standards as described previously (18). Three biological replicates of each leaf sample were used. Following extraction from plant tissues, 10 µl of the extracts were injected for analysis with an LC-MS/MS (18). LC-MS/MS analysis were achieved using a PE Sciex 3000 triple quad mass spectrometer equipped with a CTC autosampler and Shimadzu LC-MS system. These analyses were performed at the UNC (University of North Carolina) Department of Chemistry Mass Spectrometry Core Laboratory (https://chem.unc.edu/critcl-main/criticl-mass-main/).

RNA-seq analysis

Four individual plants of each genotype (wild type, *Sldmr6-1.1* and *Sldmr6-1.2* mutants) were used for RNA sequencing. Two leaves from each plant were infiltrated with mock solution (10 mM $MgCl_2$) or *X. gardneri* suspension (OD_{600}= 0.25). Six hours after syringe infiltration, leaf samples were collected, and total RNA was extracted using the Spectrum Plant Total RNA kit (Sigma, STRN250). A total of 24 RNA sequencing libraries were prepared using the illumina TruSeq Stranded mRNA Library Prep (illumina 20020594). All libraries were sequenced as 50bp single-end reads on a HiSeq 4000 sequencing platform. Illumina adapters and low-quality reads were removed from the sequenced libraries using Trim Galore v0.6.4 (--illumina -q 20)

(bioinformatics.babraham.ac.uk). The filtered reads were aligned to the reference genome (SL 4.0) using STAR v2.6.1c (19). We used primary alignments for gene counting using FeatureCounts v1.6.3 (20), and edgeR to analyze differentially expressed genes (DEGs) (21). For two compared conditions, DEGs were defined to have $|\log_2$ Fold Change$|$ >= 1 and false discovery rate (FDR) < 0.05. We employed eggNog-mapper (22) to obtain functional annotations for ITAG 4.0, and clusterProfiler (23) to perform gene ontology enrichment tests using the functional annotations of the DEGs.

Reverse transcription-polymerase chain reaction (RT-PCR)

Expression of *SlDMR6-2* gene was evaluated by semiquantitative RT-PCR in leaves and flowers of wild type plants. The Spectrum Plant Total RNA kit (Sigma, STRN250) (with on-column DNaseI treatment) and the SuperScript III First-Strand Synthesis System (Invitrogen) were used to make cDNA from 1 µg of RNA. One microliter of cDNA was used for 24 cycles of amplification using Phusion HF polymerase (New England Biolabs). *SlAct* (Solyc03g078400) gene was used as internal control. Three biological replicates were used for each condition. The primer sequences are listed in Table S1.

Recombinant protein expression and purification

The coding sequences of SlDMR6-1, SlDMR6-2, SlDMR6-1_H212Q, SlDMR6-2_H215Q, AtDMR6 and AtDLO1 were PCR-amplified with specific primers (Table S1) and cloned into pGEM-T easy vector (Promega). These inserts were digested and subcloned into pET28a vector (Novagen) for protein expression in *E. coli*. All constructs were verified by DNA sequencing.

All six constructs were individually introduced into rosetta 2(DE3)pLysS cells, which were grown at 37°C in 2YT medium (Sigma) with appropriate antibiotics. Recombinant protein expression was induced with 0.5 mM isopropyl-β-D-thiogalactoside (IPTG), and cultures were grown overnight at 16°C. For protein purification, cells were disrupted by sonication on ice and proteins were bound to a Nickel-affinity column (HisTrap Crude FF, GE Life Sciences). Elution was carried out by sequential additions of elution buffer containing imidazole. Recombinant proteins were desalted into IEX Buffer A (20 mM Tris-HCl pH 8.0, 50 mM NaCl) using HiPrep 26/10 desalting column according to manufacturer's instructions (GE Life Sciences). Desalted proteins were loaded onto a 5 ml Q HP column and eluted with 50-1000 mM NaCl over 15 CV. Fractions containing monomeric proteins were pooled and concentrated. Protein concentrations were determined by Coomassie-based assay. Samples were sterile-filtered, flash-frozen in liquid nitrogen, and stored at -80^{o}C.

In vitro activity assays

The enzyme assay was performed according to a previously described method with some modifications (24). The reaction mixture included 50 mM MES, pH 6.5, 0.4 mM $FeSO_4$, 10 mM ascorbic acid, 1 mM 2-oxoglutarate, 10 µM salicylic acid, and 12 µg of recombinant purified protein, in a final volume of 100 µl. The ferrous sulfate ($FeSO_4$) solution was prepared in 100 mM sodium acetate, pH 5.5 and 10mM ascorbic acid. Activity assays were performed at 40°C for 60 min in open tubes with shaking (225 rpm). Reactions were initiated by addition of the enzyme and terminated by filtration through a 0.22 µM syringe filter (Millipore). Samples were then analyzed by HPLC.

HPLC quantification

HPLC separation was performed on a Shimadzu SCL-10A system with a Shimadzu RF-10A scanning fluorescence detector and a Shimadzu SPD-M10A photodiode array detector. Samples were separated on a 5-µm, 15 cm x 4.6-mm i.d. Supelcosil LC-ABZ Plus column (Supelco) preceded by a LC-ABZ Plus guard column. Prior to loading the 50-µl sample, the column was equilibrated with 15% acetonitrile in 25 mM KH_2PO_4, pH 2.5, at a flow rate of 1.0 ml/min. The concentration of acetonitrile was increased linearly to 20% over 10 minutes, followed by an increase to 43% linearly over the next 12 minutes, followed by an increase to 66% over the next 2 minutes. This was followed by isocratic flow at 66% for 5 minutes, followed by a decrease to 15% acetonitrile linearly over the next 5 minutes and isocratic flow at 15% for 3 min. 2,5-DHBA and SA were quantified using a fluorescence detector set at 320-nm excitation/449-nm emission for 2,5-DHBA and 305/407 for SA. Under these conditions, 2,5-DHBA eluted at approximately 9 minutes and SA eluted at approximately 20 minutes. HPLC-grade solvents were employed for all HPLC buffers and solutions.

Homology modeling and *in silico* ligand docking

Homology models for SlDMR6-1 (NP_001233840.2) and SlDMR6-2 (XP_004241427.1) were built using the HHpred server and the MODELLER software (25), which are available at the MPI Bioinformatics Toolkit (https://toolkit.tuebingen.mpg.de/#/). The structure of Anthocyanidin synthase (ANS) from *Arabidopsis thaliana* (26) was the selected template (PDB ID 1GP6, 35-30% sequence identity with target proteins), because it was determined in complex with the cofactor Fe(II), succinic acid and its substrate, thus representing a desirable conformational state for the ligand docking procedure. The quality of built models was evaluated using the z-DOPE score calculated by the SaliLab Model Evaluation Server (http://modbase.compbio.ucsf.edu/evaluation/),

which is lower than -1.0 for good models and between 0 and -1 for reasonable models. The models were also validated using the SAVES v5.0 service (http://servicesn.mbi.ucla.edu/SAVES/) (27).

For the *in silico* ligand docking, we used the AutoDockTools v1.5.6 (28) to add non-polar hydrogens to the ligands (naringenin or salicylic acid) and enzymes (SlDMR6-1 or SlDMR6-2), to prepare the PDBQT files, and to define the grid center and the grid box size. The stochastic search algorithm of AutoDock Vina (29) was used to dock the ligands to the substrate binding site of SlDMR6-1 or SlDMR6-2. The results that best agree with our functional data as well as with the expected positioning of the reactive atom of the ligand compared to the crystallographic structure of naringenin (26) bound at AtANS were analyzed and discussed here.

Field trial assays

Seeds were sown on February 26, 2019 and single row plots of 10 plants were established in the field on March 12, 2019 at the Gulf Coast Research and Education Center (GCREC) in Balm, FL. Experimental plots were arranged in a randomized complete block design with four replications. Tomato seedlings were transplanted into raised beds covered with reflective polyethylene mulch. Pic-Clor 60 fumigant was applied at a rate of 336,25 kg/ha. Between-bed spacing was five feet, and plants were spaced 18 inches in the row. Plants were staked and tied, and irrigation was applied through drip tape beneath the plastic mulch. A recommended fertilizer and pesticide program was followed throughout the growing season, excluding the use of SAR inducers, copper, and other bactericides. Plants were inoculated on April 19, 2019 with a four-isolate cocktail of *X. perforans* race T4 (10^6 CFU per ml of each of strains GEV904, GEV917, GEV1001, GEV1063). Individual plants were evaluated for bacterial spot disease severity on May 22, 2019 using the Horsfall-Barratt rating scale (30). Vine-ripened (breaker stage through red) fruits were harvested two times from eight plants of each plot on May 28, 2019 and June 6, 2019. Fruits were weighed and graded according to USDA standards (51.1859 of the US Standards for Grades of Fresh Tomatoes) (31). Note that small fruits are 7x7 (unmarketable), and medium, large and extra-large fruits are 6x7, 6x6 and 5x6, respectively, according to the USDA specifications (31). To calculate total marketable yield, only the medium, large and extra-large fruit categories were considered. Small fruits are unmarketable and, therefore, are not used to determine total marketable yield.

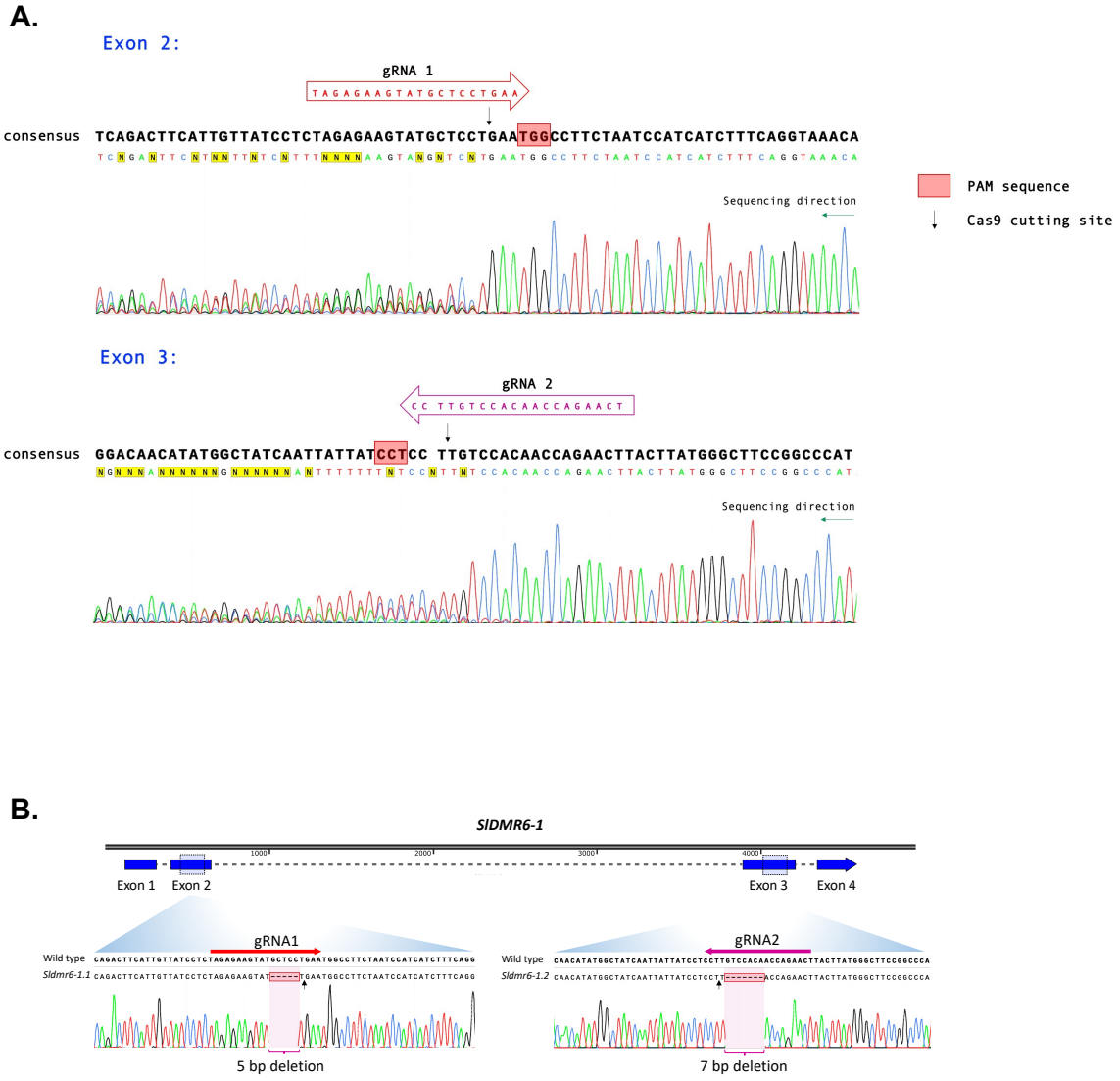

Fig. S1. Schematic representation of *SlDMR6-1* guide RNAs (gRNAs) and mutant alleles. (*A*) Two gRNAs were designed to independently target the second exon (gRNA 1) and the third exon (gRNA 2) of the *SlDMR6-1* gene. To evaluate gRNA activity, we used *Agrobacterium*-based transient expression assays in *Nicotiana benthamiana*. The target regions were sequenced, and the overlapping peaks on the chromatogram indicate that both gRNAs are active *in planta* (*B*) Two independent constructs containing gRNA 1 or gRNA 2 were used to produce stable tomato transformants. Two homozygous lines with frameshift deletion alleles, named *Sldmr6-1.1* and *Sldmr6-1.2*, were generated. The predicted cut sites of each gRNA are indicated with an arrow, and the black dashes highlighted in red correspond to the missing DNA bases that cause a frameshift in the protein sequence.

A.

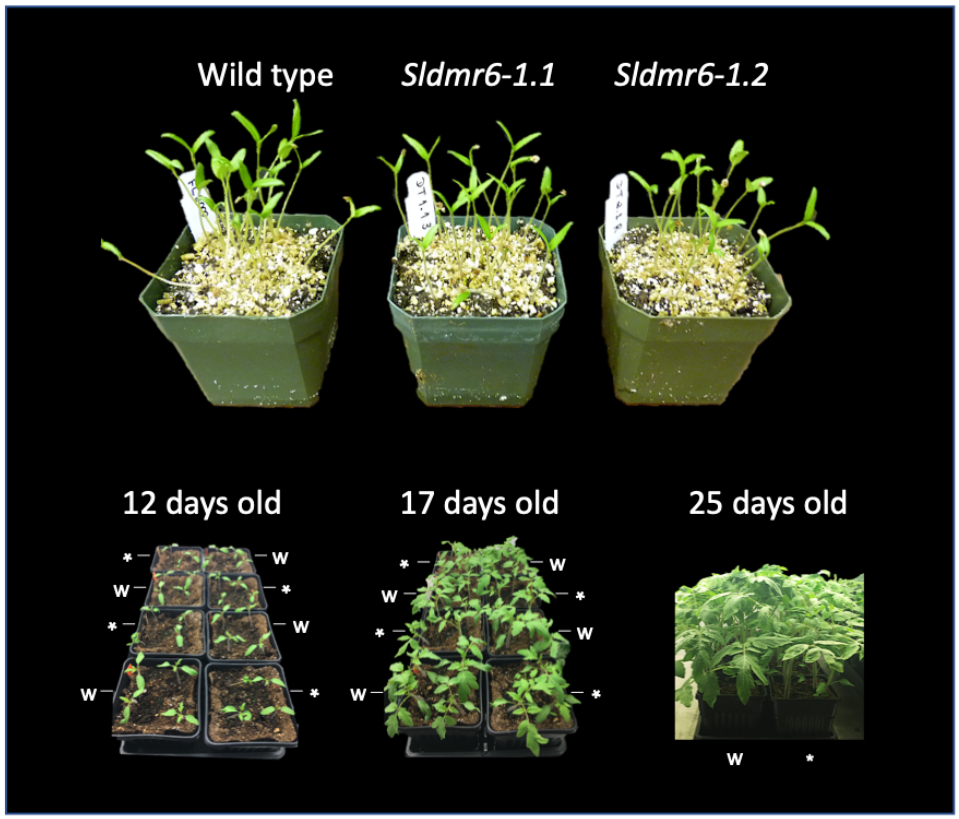

B.

Fig. S2. *SlDMR6-1* impairment does not have a clear effect on plant growth under laboratory conditions. (*A*) Growth phenotype of wild type and *Sldmr6-1* mutants grown in a growth chamber at 24°C under a 16-h light/8-h dark photoperiod and 50% relative humidity. Asterisks and letter "w" indicate *Sldmr6-1.2 mutants* and wild type lines, respectively. (*B*) Growth phenotype of wild type (Wt) and *Sldmr6-1* lines (*Sldmr6-1.2*) grown in the greenhouse at 25°C under a 16-h light/8-h dark photoperiod. *Sldmr6-1* mutants are intercalated with wild type plants.

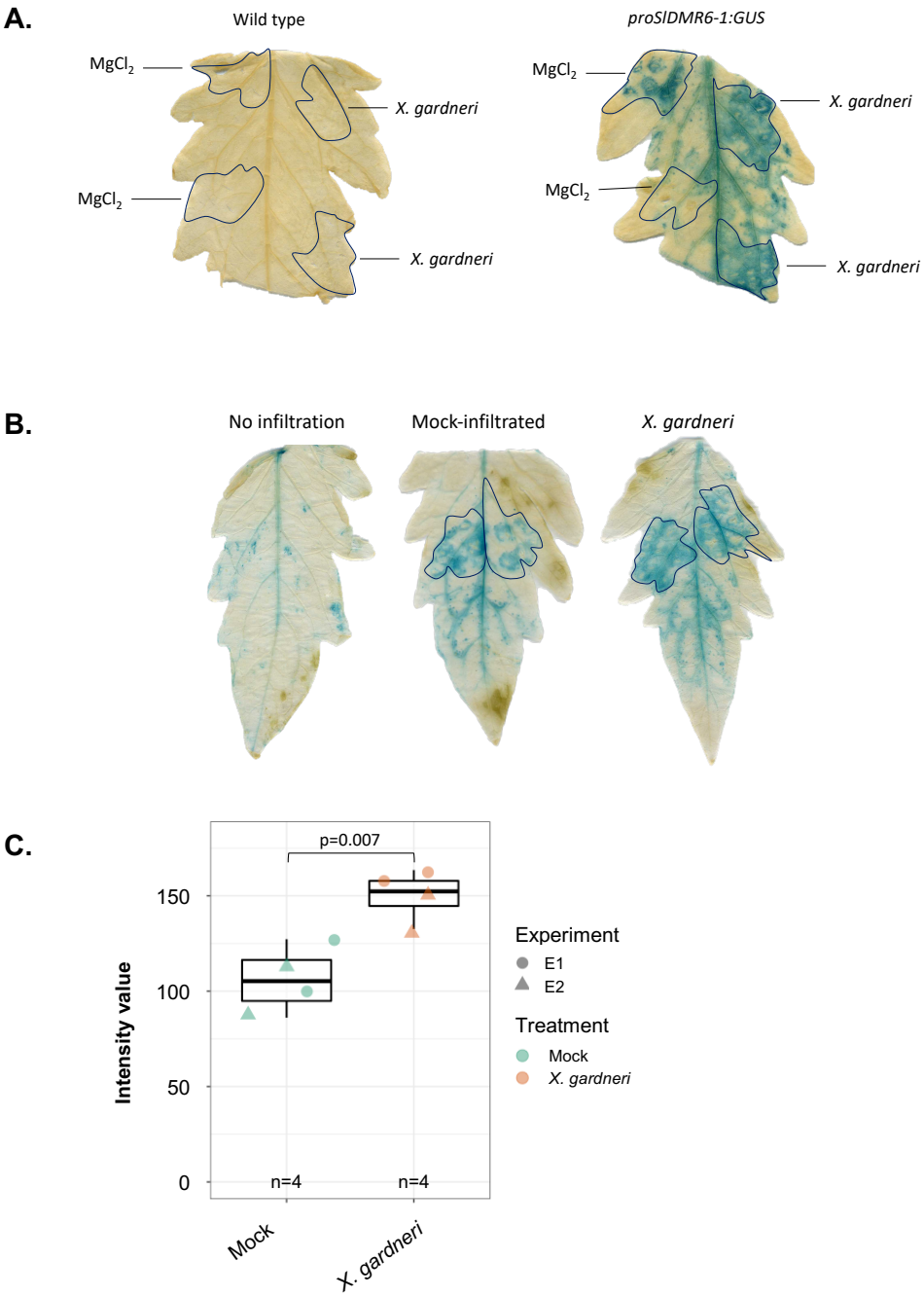

Fig. S3. Histochemical GUS assay of wild type and *proSlDMR6-1:GUS* tomato leaves in response to *Xanthomonas gardneri* 153 (*Xg*) infection. (*A*) A single leaf of the wild type or *proSlDMR6-1:GUS* line was infiltrated with mock solution on the left side and *Xg* suspension cells on the right side. (*B*) In another experimental design, leaves from the *proSlDMR6-1:GUS* line were individually submitted to three different conditions: (i) no infiltration, (ii) infiltration with mock solution (iii) infiltration with *Xg* suspension cells. GUS activity in wild type and *proSlDMR6-1:GUS* lines was visualized using X-gluc as a substrate. Based on the intensity of the GUS coloration in (*A*) and (*B*), we observed a significant infiltration effect on the *proSlDMR6-1*:*GUS* expression. Despite this, GUS staining was slightly higher in the *Xg*-infiltrated sites, confirming the up-regulation of *SlDMR6-1* by pathogen infection. Images were taken eight hours after mock or *Xg* infiltration. (*C*) Graph showing the mean GUS intensity measured within the inoculation site using the ImageJ software (32). E1 and E2 correspond to the experiments that are shown in (*A*) and (*B*), respectively.

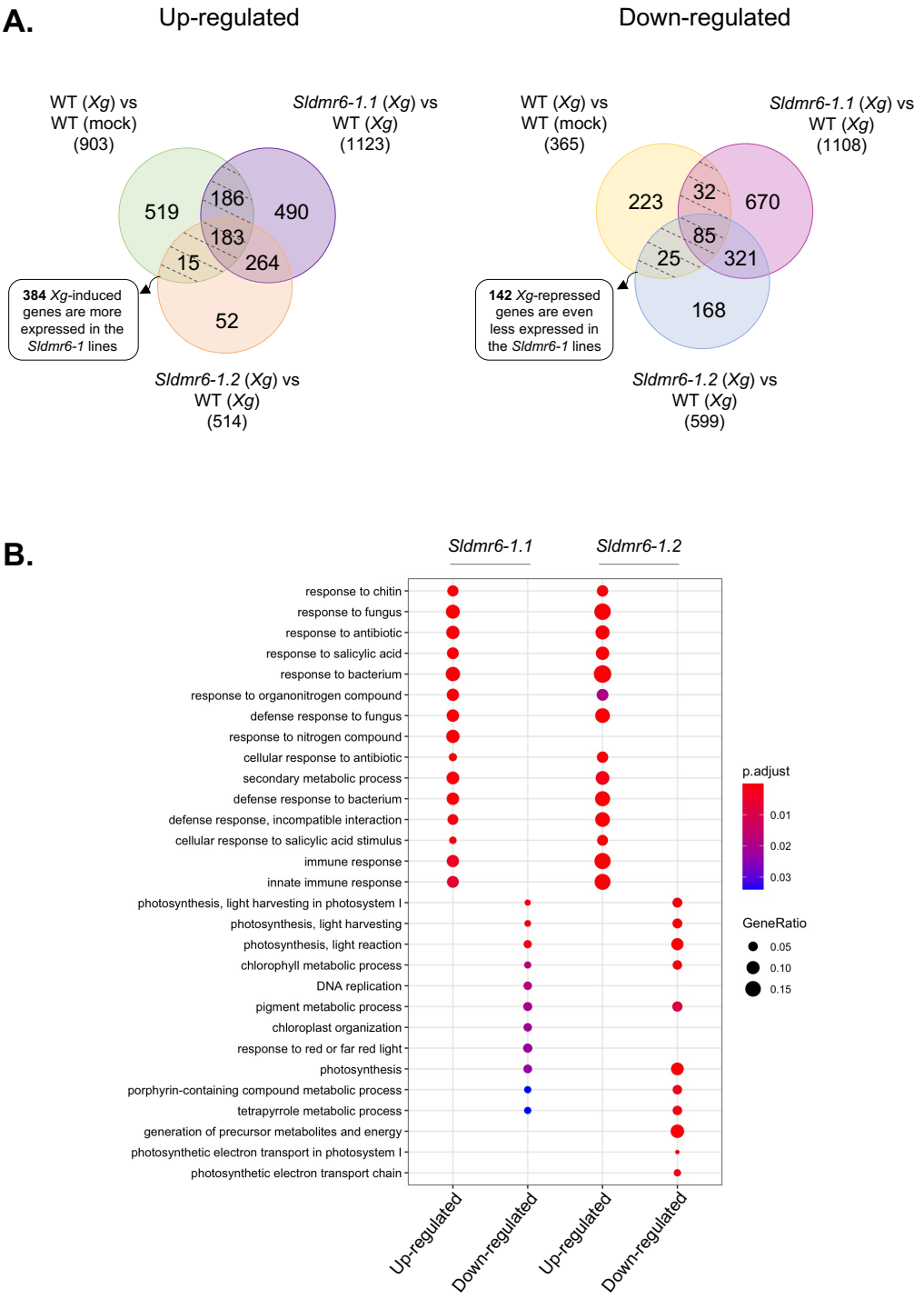

Fig. S4. Transcriptional response to *Xanthomonas gardneri* (*Xg*) infection in the wild type and *Sldmr6-1* lines (*Sldmr6-1.1* and *Sldmr6-1.2*). (*A*) Venn diagram showing *Xg*-responsive genes (Wt-*Xg* vs Wt-mock) that are up-regulated in the *Sldmr6-1* lines in comparison to wild type plants (left panel) and *Xg*-responsive genes (Wt-*Xg* vs Wt-mock) that are down-regulated in the *Sldmr6-1* lines in comparison to wild type plants (right panel). Notably, the expression of many *Xg*-induced genes (left panel) is higher in the *Sldmr6-1* lines than in wild type plants, whereas the expression of several *Xg*-repressed genes (right panel) is even lower in the mutants. (*B*) Gene Ontology (GO) analyses showed that the up-regulated genes of the infected *Sldmr6-1* mutants are enriched in GO terms associated with plant immunity, while down-regulated genes of the infected *Sldmr6-1* mutants are enriched in GO terms related to photosynthetic processes.

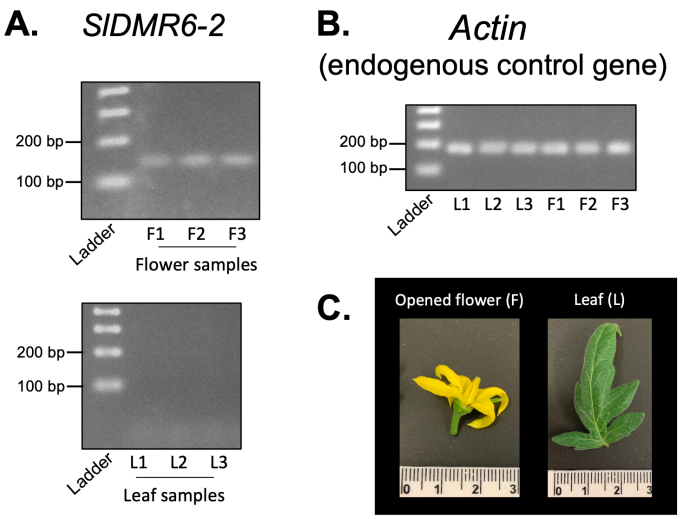

Fig. S5. Expression of the *SlDMR6-2* gene is detected in flowers (F) but not in leaf tissues (L) of wild type tomato plants. (*A*) *SlDMR6-2* expression was evaluated by RT-PCR in flowers and leaves of tomato. In agreement with our analysis of public transcriptome data, *SlDMR6-2* expression is detected in flowers but not in leaf tissues. (*B*) *SlAct* (Solyc03g078400) was used as internal control since it shows very similar expression levels in both tomato tissues. (*C*) Representative image of the tissues collected for RT-PCR analysis, opened flowers (F) and leaves (L).

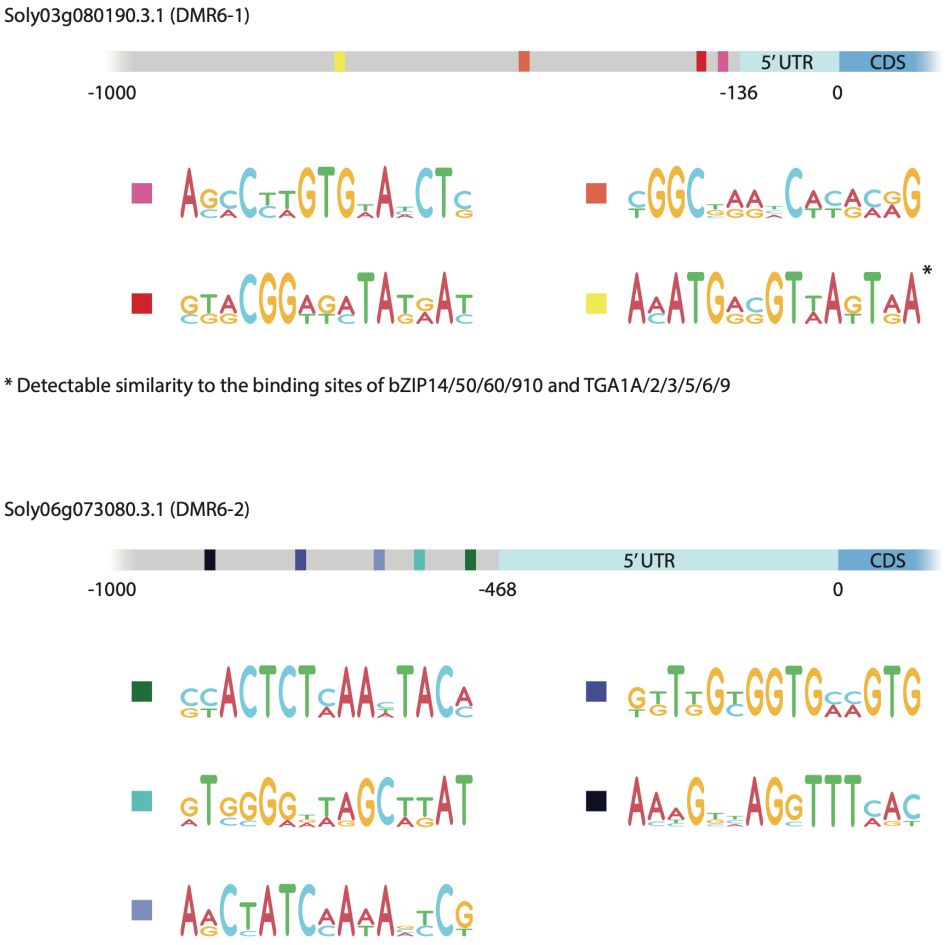

Fig. S6. Comparison of the *SlDMR6-1* and *SlDMR6-2* promoter regions. The 1-kb upstream regions of *SlDMR6-1*, *SlDMR6-2* and their respective orthologs were collected from tomato (*Solanum lycopersicum*), *Solanum pennellii*, pepper (*Capsicum annuum*), *Capsicum baccatum*, *Petunia axillaris* and *Petunia inflata*. Conserved DNA motifs located outside the UTR inferred from the cDNA data were selected and annotated. Comparison of the similarity of the chosen motifs with known transcription binding sites revealed that the *SlDMR6-1* promoter has a motif with similarity to the binding sites of several basic leucine zipper (bZIP) TGA transcription factors (p-value < 0.001).

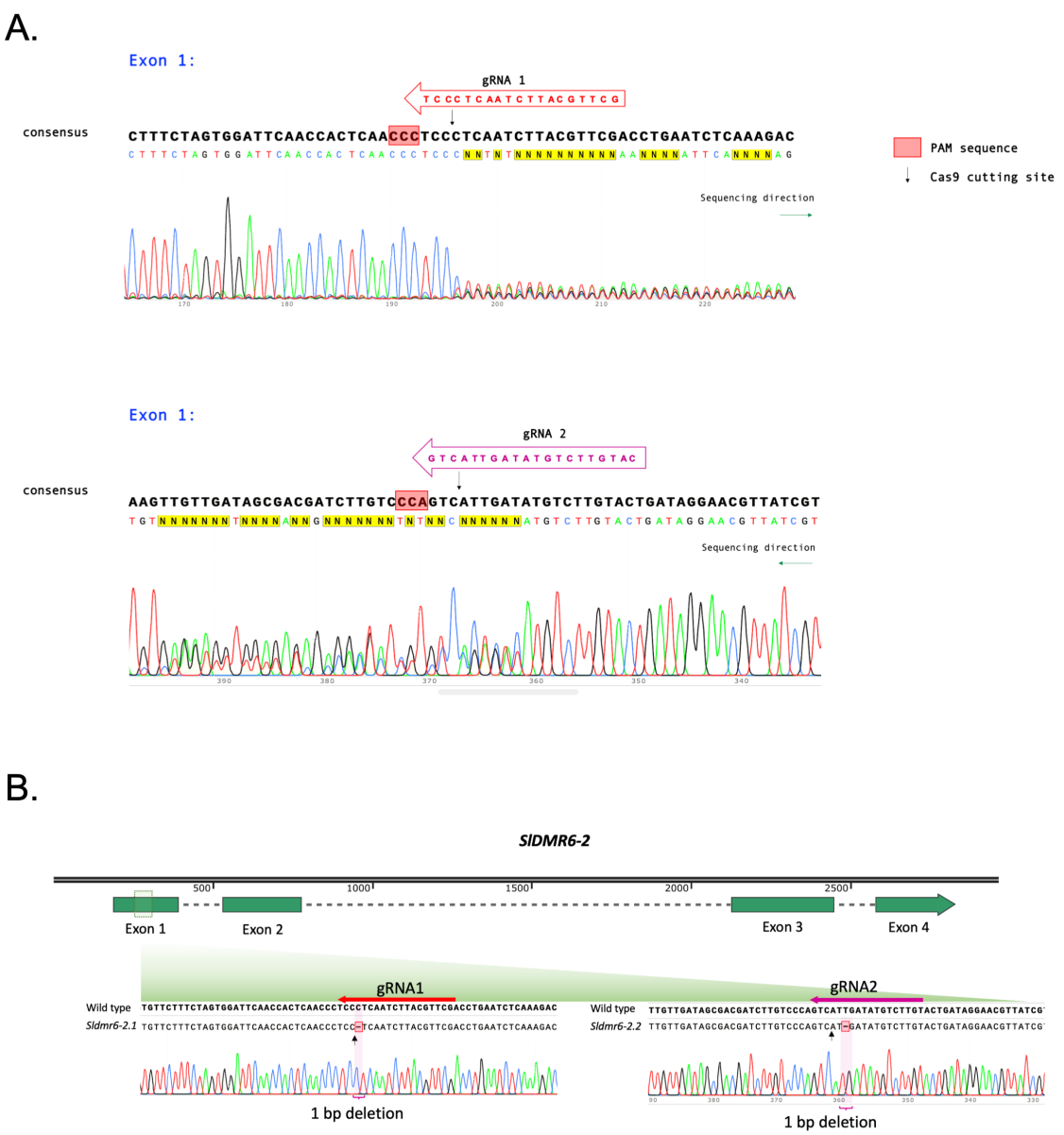

Fig. S7. *SlDMR6-2* guide RNAs (gRNAs) and mutant alleles. (*A*) Evaluation of gRNA activity using an *Agrobacterium*-based transient expression assay in *Nicotiana benthamiana*. Selected gRNAs (gRNA1 and gRNA2) target different regions of the first exon of the *SlDMR6-2* gene. The target regions were sequenced, and the mixed sequencing results confirm the activity of both gRNAs *in planta*. (*B*) Two independent constructs containing gRNA 1 or gRNA 2 were used to generate stable tomato transformants. Two homozygous lines with frameshift deletion alleles were produced: *Sldmr6-2.1* and *Sldmr6-2.2*. The predicted cleavage sites for each gRNA are indicated by an arrow, and the black dashes highlighted in red correspond to the missing DNA bases that cause the frameshift in the protein sequence.

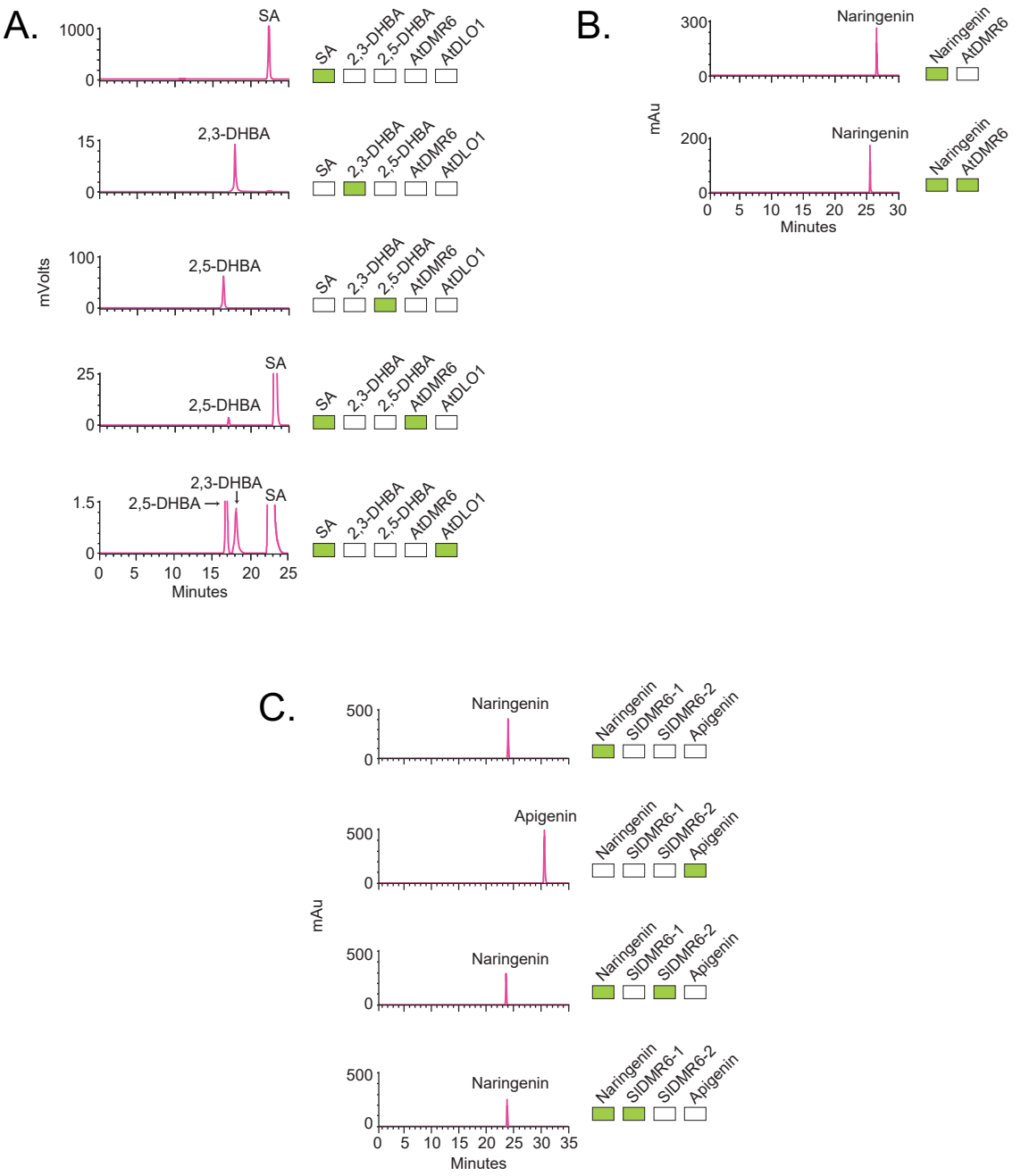

Fig. S8. AtDLO1 and AtDMR6 are salicylic acid (SA)-hydroxylase enzymes, and SlDMR6-1 and SlDMR6-2 do not show flavone synthase (FNS) activity. (*A*) HPLC profiles of the standards SA, 2,3-DHBA and 2,5-DHBA (first, second and third panels, respectively). In the presence of the recombinant protein AtDMR6, SA is converted to 2,5 DHBA, whereas, in the presence of AtDLO1, SA is converted to 2,3-DHBA and 2,5 DHBA (fourth and fifth panels, respectively). These results agree with previous literature data (18, 24). (*B*) HPLC profile of the standard naringenin (first panel). AtDMR6 is not able to use naringenin as a substrate under the tested conditions. (*C*) HPLC profile of the standard naringenin (first panel) and apigenin (second panel). Similar to AtDMR6 (24), SlDMR6-1 and SlDMR6-2 are not able to use naringenin as a substrate under the tested conditions (third and fourth panels). The green boxes indicate the presence of that compound in the reaction mixture.

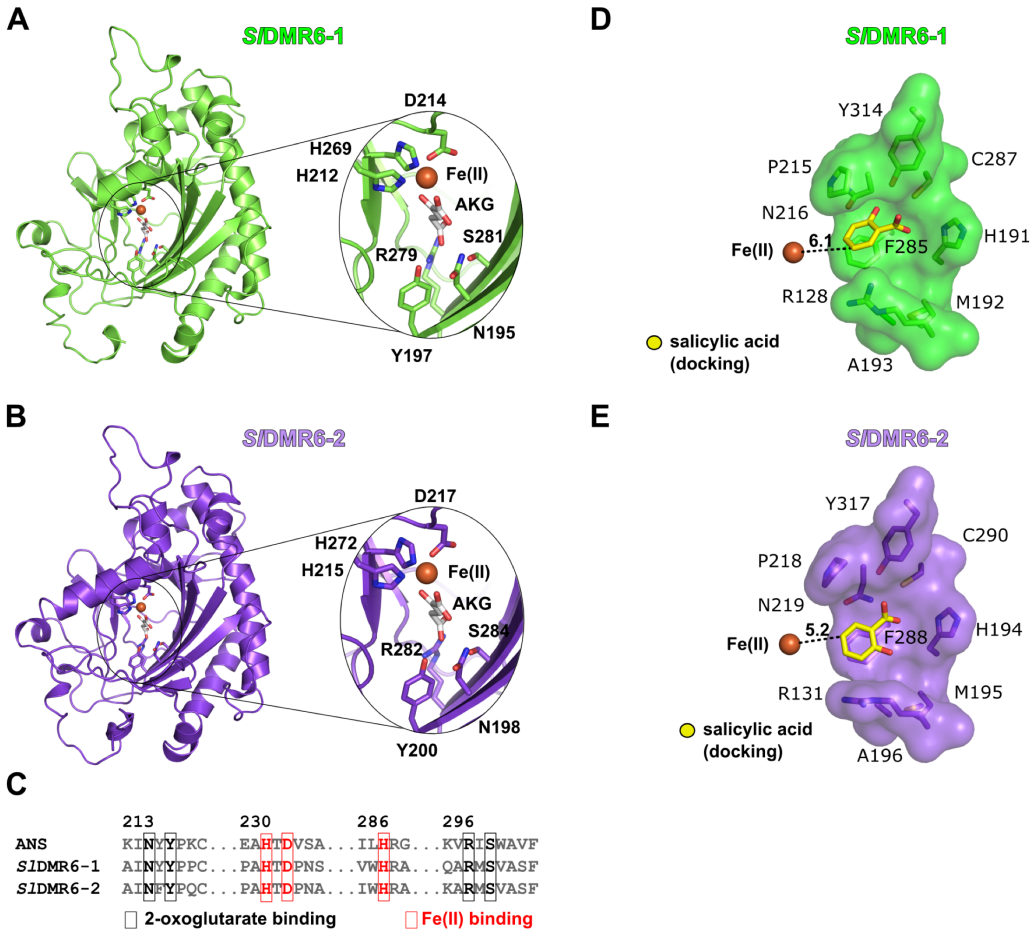

Fig. S9. Homology models of SlDMR6-1 and 2 show conserved features of 2-oxoglutarate Fe(II)-dependent dioxygenase (2-ODD) enzymes and a substrate-binding site that accommodates salicylic acid (SA). The SlDMR6-1 (*A*) and SlDMR6-2 (*B*) models were built using anthocyanidin synthase (ASN) as a template and displayed a z-DOPE score of -1.163 and -0.892, respectively. Magnified views highlight the conserved residues that bind to 2-oxoglutarate (AKG) and Fe(II), numbered according to their position in the respective enzyme sequence. Fe(II) and AKG coordinates were from the PDB 2BRT (33) superimposed to the SlDMR6 models. (*C*) Sequence alignment between ANS, SlDMR6-1, and SlDMR6-2 highlighting the conserved residues displayed in panels (*A*) and (*B*). Numbers correspond to amino acid positions in ANS. Molecular docking of SA into the substrate-binding site of SlDMR6-1 (*D*) and SlDMR6-2 (*E*) indicates two possible fits that place the C-5 carbon atom at a distance (dashed lines, Å) from Fe(II) similar to that find between Fe(II) and the reactive position (C-3 atom from central ring) of naringenin bound to ANS crystal structure (6.4 Å).

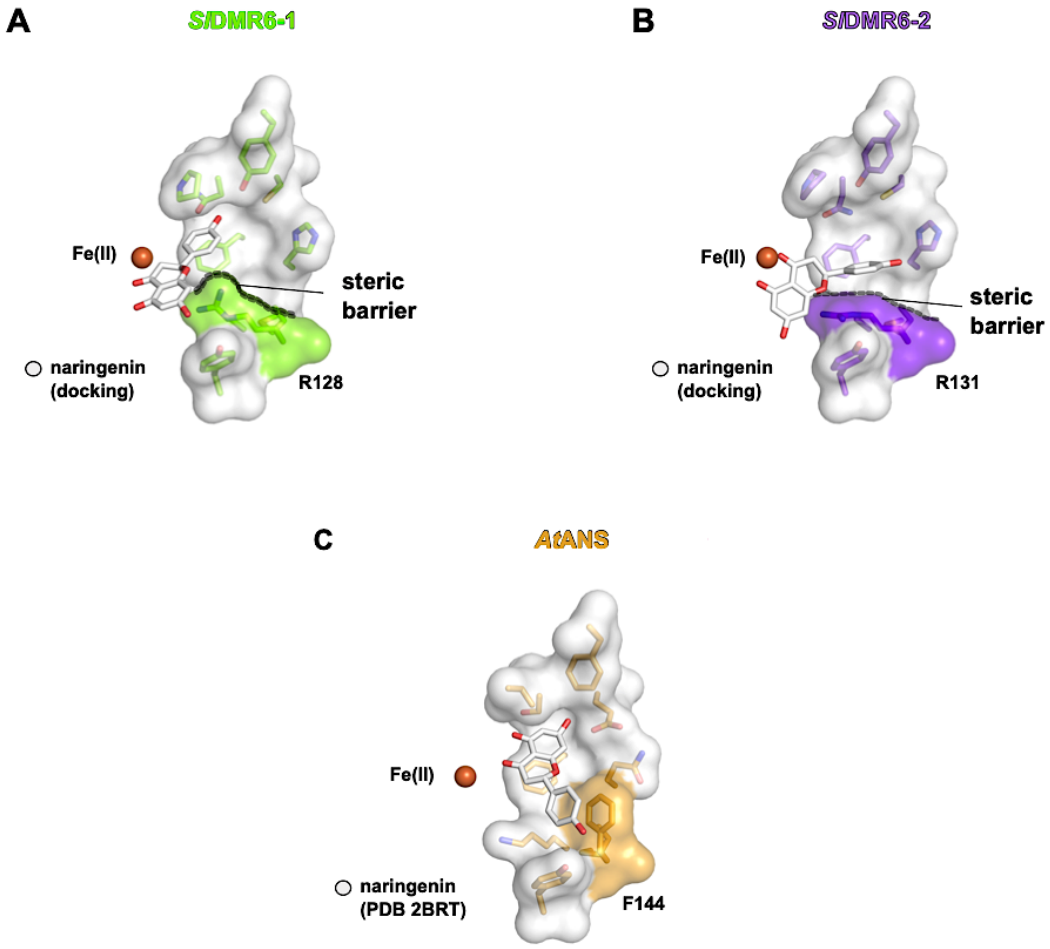

Fig. S10. An arginine residue conserved in DMR6 enzymes probably prevents naringenin to occupy the same position as it does in AtANS. Panels (*A*) and (*B*) show molecular docking results of naringenin at the active site of homology models of SlDMR6-1 and SlDMR6-2, respectively. Panel (*C*) presents the crystal structure of AtANS-Fe(II)-alpha-ketoglutarate (AKG)-naringenin complex (33). Residues equivalent to SlDMR6-1-Arg128 are highlighted by colored surfaces. Fe(II) and AKG coordinates were from the PDB 2BRT (33) superimposed to the respective homology models shown in panels (*A*), (*B*) and (*C*).

A.

B.

Fig. S11. Growth phenotype of wild type and *Sldmr6-1* plants under field conditions. (*A*) Wild type and *Sldmr6-1* (*Sldmr6-1.1*) mutants growing under field conditions in Florida. (*B*) Individual plants of the wild type and *Sldmr6-1* (*Sldmr6-1.1*) genotypes showing the main differences in growth verified when the mutants were grown in the field. The *Sldmr6-1* lines are slightly stunted, and this trait affects the entire plant, including height, internode length and leaf size. It is worth mentioning that naturally existing *Xanthomonas* are always present in Florida, thus it is still necessary to evaluate the effect of *SlDMR6-1* mutation on healthy uninfected plants growing in the field.

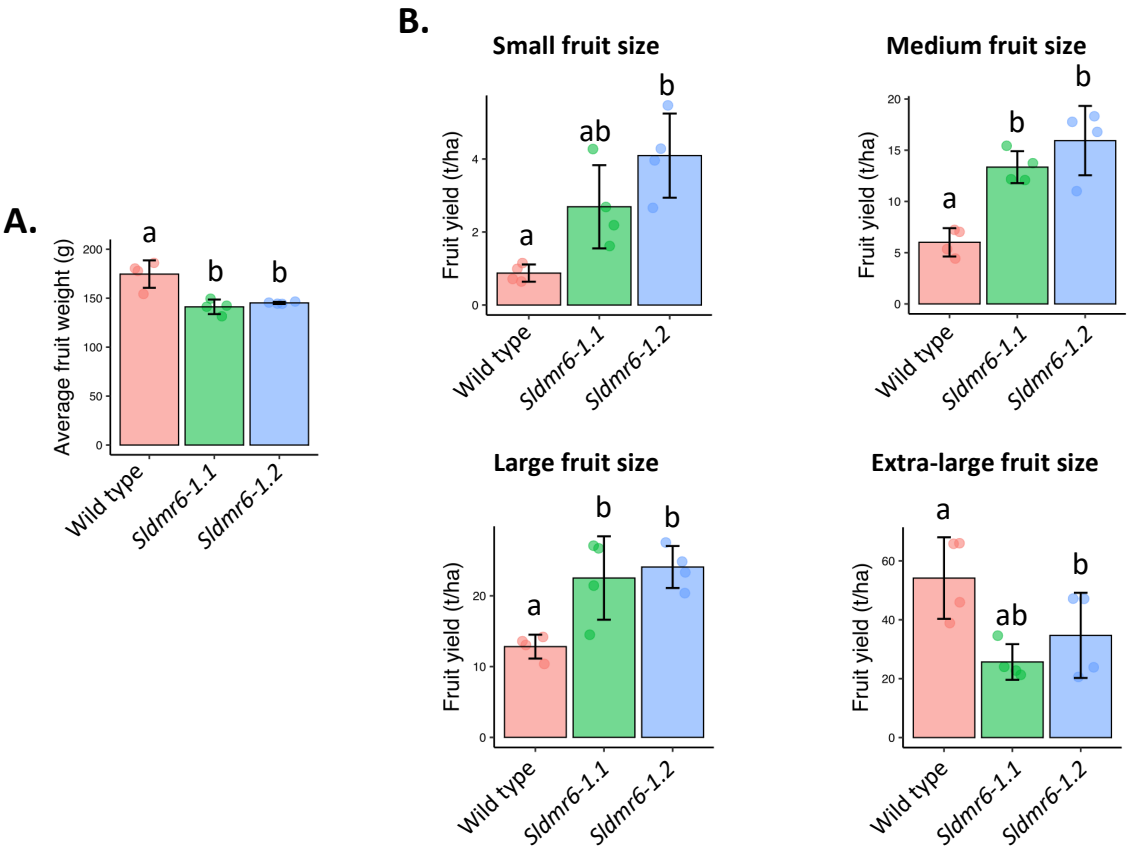

Fig. S12. Impact of the *SlDMR6-1* mutation on average fruit weight and yield (*A*) Comparison of the average fruit weight of the wild type and the mutant lines *Sldmr6-1.1* and *Sldmr6-1.2*. Average fruit weight includes the following fruit size categories: extra-large, large, and medium fruits. (*B*) Yield of the different tomato fruit categories. Small fruits are unmarketable and, therefore, are not used to determine total marketable yield. Both mutants show reduced yield of extra-large fruits, but higher yield of large and medium fruits. As a result, total marketable yield is not altered (Fig. 6C). The letters indicate significant difference between the conditions as determined using a one-way ANOVA followed by a Tukey HSD test ($p < 0.05$).

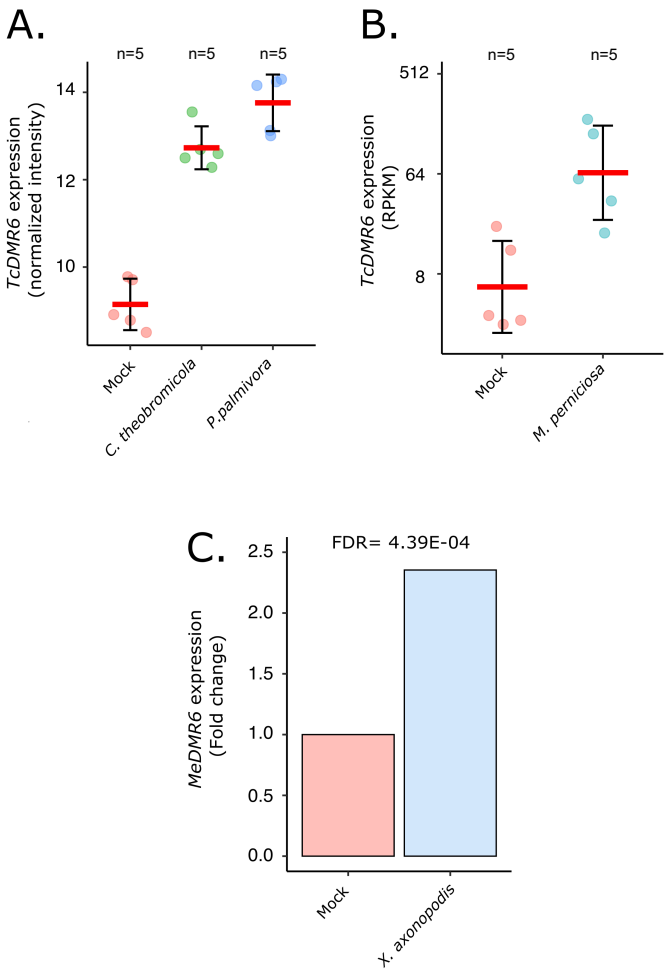

Fig. S13. Expression of *AtDMR6* orthologs in *Theobroma cacao* (cacao) and *Manihot esculenta* (cassava). (*A*) Upregulation of *TcDMR6* (Thecc1EG015521t1) in response to *Colletotrichum theobromicola*, *Phytophthora palmivora* and *Moniliophthora perniciosa* based on the analysis of public transcriptome data (FDR < 0.05) (7, 9). (*B*) Similarly, *MeDMR6* (Manes.01G043500.1) is also induced by pathogen infection (*Xanthomonas axonopodis* pv. *manihotis*) (n=3) (8).

406 **Table S1.** Primer sequences

Primer names	Sequences (5'- 3')	Purpose
SlDMR6-1_Exon2_F	ATGGTGTACCAAAGGAAGTTGTAGAGA	Forward primer to amplify a fragment of exon 2 of the *SlDMR6-1* gene for the Agrobacterium-based transient expression assays and for plant genotyping
SlDMR6-1_Exon2_R	TGCAACACTTCTCAGTTTGAGCCTCG	Reverse primer to amplify a fragment of exon 2 of the *SlDMR6-1* gene for the Agrobacterium-based transient expression assays and for plant genotyping
SlDMR6-1_Exon3_F	AGATATTGCAGGGAAATTCGTCAACTC	Forward primer to amplify a fragment of exon 3 of the *SlDMR6-1* gene for the Agrobacterium-based transient expression assays and for plant genotyping
SlDMR6-1_Exon3_R	GATGCCATACACTTCTGTACTTACCGTT	Reverse primer to amplify a fragment of exon 3 of the *SlDMR6-1* gene for the Agrobacterium-based transient expression assays and for plant genotyping
SlDMR6-1_gRNA1_F	ATTGTAGAGAAGTATGCTCCTGAA	Forward primer for cloning *SlDMR6-1* gRNA1
SlDMR6-1_gRNA1_R	AAACTTCAGGAGCATACTTCTCTA	Reverse primer for cloning *SlDMR6-1* gRNA1
SlDMR6-1_gRNA2_F	ATTGAGTTCTGGTTGTGGACAAGG	Forward primer for cloning *SlDMR6-1* gRNA2
SlDMR6-1_gRNA2_R	AAACCCTTGTCCACAACCAGAACT	Reverse primer for cloning *SlDMR6-1* gRNA2
SlDMR6-2_Exon1_F	ATCAAGTCAGTAAAATGTGAACC	Forward primer to amplify a fragment of exon 1 of the *SlDMR6-2* gene for the Agrobacterium-based transient expression assays and for plant genotyping
SlDMR6-2_Exon1_R	CTCTCCAATTATGAACAGTTTCC	Reverse primer to amplify a fragment of exon 1 of the *SlDMR6-2* gene for the Agrobacterium-based transient expression assays and for plant genotyping
SlDMR6-2_gRNA1_F	ATTGTCGAACGTAAGATTGAGGGA	Forward primer for cloning *SlDMR6-2* gRNA1
SlDMR6-2_gRNA1_R	AAACTCCCTCAATCTTACGTTCGA	Reverse primer for cloning *SlDMR6-2* gRNA1
SlDMR6-2_gRNA2_F	ATTGGTACAAGACATATCAATGAC	Forward primer for cloning *SlDMR6-2* gRNA2

SlDMR6-2_gRNA2_R	AAACGTCATTGATATGTCTTGTAC	Reverse primer for cloning *SlDMR6-2* gRNA2
Cas9_F	ACAGAGAGATGATCGAGGAACGG	Forward primer to amplify the *Cas9* gene for genotyping
Cas9_R	AGTTCCTGGTCCACGTACATATCC	Reverse primer to amplify the *Cas9* gene for genotyping
SlAct_qPCR_F	TGTTCTCCTGACTGAGGCACC	*SlAct* forward primer to perform the qPCR analysis
SlAct_qPCR_R	GACTAACACCATCACCAGAGTCC	*SlAct* reverse primer to perform the qPCR analysis
SlDMR6-1_qPCR_F	ATTCAGATGATCCTTCAAAGACC	*SlDMR6-1* forward primer to perform the qPCR analysis
SlDMR6-1_qPCR_R	GAATTTCCCTGCAATATCTGC	*SlDMR6-1* reverse primer to perform the qPCR analysis
GUS_F	CTGTGGAATTGATCAGCGTTGG	Forward primer to amplify the reporter gene *GUS*
GUS_R	CTCCATCACTTCCTGATTATTGACCC	Reverse primer to amplify the reporter gene *GUS*
Pro_SlDMR6-1_F	CACCTTGTTAGTGATATCTGTTGGC	Forward primer to amplify a 2.5 fragment of the *SlDMR6-1* gene
Pro_SlDMR6-1_R	GGAATCTATGGCTTATAATATATATGG	Reverse primer to amplify a 2.5 fragment of the *SlDMR6-1* gene
SlAct_RT_F	TGTTCTCCTGACTGAGGCACC	Forward primer to amplify the *SlAct* gene by RT-PCR
SlAct_RT_R	GACTAACACCATCACCAGAGTCC	Reverse primer to amplify the *SlAct* gene by RT-PCR
SlDMR6-2_RT_F	TAGGCTACATTGTTATCCTTTGG	Forward primer to amplify the *SlDMR6-2* gene by RT-PCR
SlDMR6-2_RT_R	CCTAAGCTCTCTGATATTGC	Reverse primer to amplify the *SlDMR6-2* gene by RT-PCR
AtDMR6_pET28a_F	GCTAGCATGGCGGCAAAGCTGATATC	Forward primer to amplify and clone the complete *AtDMR6* coding sequence
AtDMR6_pET28a_R	GAATTCTTAGTTGTTTAGAAAATTCTCGAGGC	Reverse primer to amplify and clone the complete *AtDMR6* coding sequence
AtDLO1_pET28a_F	GCTAGCATGGCAACTTCTGCAATATCTAAG	Forward primer to amplify and clone the complete *AtDLO1* coding sequence
AtDLO1_pET28a_R	GAATTCTTAGGTTGTTGGAGCTTTGAAG	Reverse primer to amplify and clone the complete *AtDLO1* coding sequence
SlDMR6-2_pET28a_F	TACGTGGATCCATGATGACAACAACAAGTGTTCTTTC	Forward primer to amplify and clone the complete *SlDMR6-2* coding sequence

SlDMR6-2_pET28a_R	TCTACGAATTCTTAGGTTCCATCGTTCTTAAAAAG	Reverse primer to amplify and clone the complete *SlDMR6-2* coding sequence
SlDMR6-1_pET28a_F	TACGTGGATCCATGGAAACCAAAGTTATTTCTAGC	Forward primer to amplify and clone the complete *SlDMR6-1* coding sequence
SlDMR6-1_pET28a_R	TCTACGAGCTCTTAGTTCTTGAAAAGTTCCAAAC	Reverse primer to amplify and clone the complete *SlDMR6-1* coding sequence

407
408

Table S2. Effect of *SlDMR6-1* mutation and *Xanthomonas gardneri* 153 (*Xg*) infection in the number of differentially expressed genes (DEGs)

Comparisons		Up-regulated	Down-regulated	Total DEGs
Sldmr6-1.2 Mock	*Sldmr6-1.1* Mock	13	11	24
Sldmr6-1.2 Xg	*Sldmr6-1.1 Xg*	16	20	36
Sldmr6-1.1 Mock	Wild type Mock	760	514	1274
Sldmr6-1.1 Xg	Wild type *Xg*	1123	1108	2231
Sldmr6-1.2 Mock	Wild type Mock	523	328	851
Sldmr6-1.2 Xg	Wild type *Xg*	514	599	1113
Wild type *Xg*	Wild type Mock	903	365	1268
Sldmr6-1.1 Xg	*Sldmr6-1.1* Mock	1149	926	2075
Sldmr6-1.2 Xg	*Sldmr6-1.2* Mock	1079	969	2048

FDR <0.05 and |log2 (Fold change)| ≥1

Dataset 1 (separate file). Differentially expressed genes (DEGs) between wild type and *Sldmr6-1* mutants.

Dataset 2 (separate file). Gene Ontology (GO) terms that are enriched among DEGs of the *Sldmr6-1* mutant lines.

Dataset 3 (separate file). Differentially expressed genes (DEGs) of wild type and *Sldmr6-1* mutants in response to *Xanthomonas gardneri* (*Xg*) infection.

Dataset 4 (separate file). Comparison of the transcriptomes of the wild type, *Sldmr6-1.1* and *Sldmr6-1.2* tomato lines during *Xanthomonas gardneri* infection

Dataset 5 (separate file). Composition, gene ontology (GO) enrichment analysis and annotation of each cluster obtained in the hierarchical clustering analysis of Figure 3.

SI References

1. C. Camacho, *et al.*, BLAST+: architecture and applications. *BMC Bioinformatics* **10**, 421 (2009).

2. K. Katoh, D. M. Standley, MAFFT multiple sequence alignment software version 7: improvements in performance and usability. *Mol Biol Evol* **30**, 772–780 (2013).

3. A. Stamatakis, RAxML version 8: a tool for phylogenetic analysis and post-analysis of large phylogenies. *Bioinformatics* **30**, 1312–1313 (2014).

4. J. Jupe, *et al.*, *Phytophthora capsici*-tomato interaction features dramatic shifts in gene expression associated with a hemi-biotrophic lifestyle. *Genome Biol* **14**, R63 (2013).

5. Y.-X. Yang, *et al.*, RNA-seq analysis reveals the role of red light in resistance against *Pseudomonas syringae* pv. *tomato* DC3000 in tomato plants. *BMC Genomics* **16**, 120 (2015).

6. J. L. Costa, *et al.*, *Moniliophthora perniciosa* , the causal agent of witches' broom disease of cacao, interferes with cytokinin metabolism during infection of Micro-Tom tomato and promotes symptom development. *New Phytologist*, nph.17386 (2021).

7. A. S. Fister, *et al.*, Theobroma cacao L. pathogenesis-related gene tandem array members show diverse expression dynamics in response to pathogen colonization. *BMC Genomics* **17**, 363 (2016).

8. M. Cohn, *et al.*, *Xanthomonas axonopodis* Virulence Is Promoted by a Transcription Activator-Like Effector–Mediated Induction of a SWEET Sugar Transporter in Cassava. *MPMI* **27**, 1186–1198 (2014).

9. P. J. P. L. Teixeira, *et al.*, High-Resolution Transcript Profiling of the Atypical Biotrophic Interaction between *Theobroma cacao* and the Fungal Pathogen *Moniliophthora perniciosa*. *Plant Cell* **26**, 4245–4269 (2014).

10. T. L. Bailey, *et al.*, MEME SUITE: tools for motif discovery and searching. *Nucleic Acids Res* **37**, W202–W208 (2009).

11. A. Khan, *et al.*, JASPAR 2018: update of the open-access database of transcription factor binding profiles and its web framework. *Nucleic Acids Research* **46**, D260–D266 (2018).

12. S. Kunwar, *et al.*, Transgenic expression of *EFR* and *Bs2* genes for field management of bacterial wilt and bacterial spot of tomato. *Phytopathology* **108**, 1402–1411 (2018).

13. A. Schultink, T. Qi, A. Lee, A. D. Steinbrenner, B. Staskawicz, *Roq1* mediates recognition of the *Xanthomonas* and *Pseudomonas* effector proteins *XopQ* and *HopQ1*. *Plant J* **92**, 787–795 (2017).

14. T. Qi, *et al.*, NRG1 functions downstream of EDS1 to regulate TIR-NLR-mediated plant immunity in *Nicotiana benthamiana*. *Proc Natl Acad Sci USA* **115**, E10979–E10987 (2018).

15. P. Hajdukiewicz, Z. Svab, P. Maliga, The small, versatilepPZP family ofAgrobacterium binary vectors for plant transformation. *Plant Mol Biol* **25**, 989–994 (1994).

16. T. Nakagawa, *et al.*, Development of series of gateway binary vectors, pGWBs, for realizing efficient construction of fusion genes for plant transformation. *Journal of Bioscience and Bioengineering* **104**, 34–41 (2007).

17. R. A. Jefferson, Assaying chimeric genes in plants: The *GUS* gene fusion system. *Plant Mol Biol Rep* **5**, 387–405 (1987).

18. K. Zhang, R. Halitschke, C. Yin, C.-J. Liu, S.-S. Gan, Salicylic acid 3-hydroxylase regulates *Arabidopsis* leaf longevity by mediating salicylic acid catabolism. *Proc Natl Acad Sci USA* **110**, 14807–14812 (2013).

19. A. Dobin, *et al.*, STAR: ultrafast universal RNA-seq aligner. *Bioinformatics* **29**, 15–21 (2013).

20. Y. Liao, G. K. Smyth, W. Shi, featureCounts: an efficient general purpose program for assigning sequence reads to genomic features. *Bioinformatics* **30**, 923–930 (2014).

21. M. D. Robinson, D. J. McCarthy, G. K. Smyth, edgeR: a Bioconductor package for differential expression analysis of digital gene expression data. *Bioinformatics* **26**, 139–140 (2010).

22. J. Huerta-Cepas, *et al.*, Fast genome-wide functional annotation through orthology assignment by eggNOG-mapper. *Molecular Biology and Evolution* **34**, 2115–2122 (2017).

23. G. Yu, L.-G. Wang, Y. Han, Q.-Y. He, clusterProfiler: an R package for comparing biological themes among gene clusters. *OMICS: A Journal of Integrative Biology* **16**, 284–287 (2012).

24. Y. Zhang, *et al.*, *S5H/DMR6* encodes a salicylic acid 5-hydroxylase that fine-tunes salicylic acid homeostasis. *Plant Physiol* **175**, 1082–1093 (2017).

25. B. Webb, A. Sali, Comparative protein structure modeling using MODELLER. *Curr Protoc Bioinformatics* **54** (2016).

26. R. C. Wilmouth, *et al.*, Structure and mechanism of anthocyanidin synthase from *Arabidopsis thaliana*. *Structure* **10**, 93–103 (2002).

27. M. Shen, A. Sali, Statistical potential for assessment and prediction of protein structures. *Protein Sci* **15**, 2507–2524 (2006).

28. G. M. Morris, *et al.*, AutoDock4 and AutoDockTools4: Automated docking with selective receptor flexibility. *J Comput Chem* **30**, 2785–2791 (2009).

29. O. Trott, A. J. Olson, AutoDock Vina: Improving the speed and accuracy of docking with a new scoring function, efficient optimization, and multithreading. *J Comput Chem*, NA-NA (2009).

30. J. G. Horsfall, R. W. Barratt, An improved grading system for measuring plant diseases. *Phytopathology* **35**, 655 (1945).

31. USDA, United States standards for grades of fresh tomatoes. *United States Department of Agriculture* (1991).

32. C. Béziat, J. Kleine-Vehn, E. Feraru, “Histochemical Staining of β-Glucuronidase and Its Spatial Quantification” in *Plant Hormones*, Methods in Molecular Biology., J. Kleine-Vehn, M. Sauer, Eds. (Springer New York, 2017), pp. 73–80.

33. R. W. D. Welford, I. J. Clifton, J. J. Turnbull, S. C. Wilson, C. J. Schofield, Structural and mechanistic studies on anthocyanidin synthase catalysed oxidation of flavanone substrates: the effect of C-2 stereochemistry on product selectivity and mechanism. *Org Biomol Chem* **3**, 3117 (2005).